Research articles

Influence of the low local symmetry of Er^{3+} ions on magnetic circular dichroism and absorption spectra of *f-f* transitions in $ErFe_3(BO_3)_4$ single crystal

A.V. Malakhovskii*, V.V. Sokolov, I.A. Gudim

Kirensky Institute of Physics, Federal Research Center KSC SB RAS, 660036 Krasnoyarsk, Russian Federation

ABSTRACT

Linearly polarized absorption spectra and magnetic circular dichroism (MCD) spectra of $ErFe_3(BO_3)_4$ single crystal were measured in the range of 9000–23000 cm^{-1} at 90 K. The absorption spectra of *f-f* transitions were decomposed into the Lorentz shape components and intensities of the components were found. MCD spectra permitted us to measure the Zeeman splitting of some transitions and so to determine changes of the Landé factor along the C_3 axis of the crystal during these transitions. Optical and magneto-optical properties of *f-f* transitions in the $ErFe_3(BO_3)_4$ crystal were compared with those in the $ErAl_3(BO_3)_4$ crystal. Substantial difference of the properties connected with the difference of the Er^{3+} ions local symmetry in two crystals was revealed. Large splitting of one of the *f-f* transitions without magnetic field, which is not possible for the Kramers doublets, was observed. It was explained by appearance of two absorbing centers due to the local decrease of symmetry in the excited state. Appreciable difference of the local vibrations energy in some excited states was revealed.

1. Introduction

In the high temperature phase ferroborates of the $RFe_3(BO_3)_4$ type (R–rare earth (RE) metal) have huntite-like structure with the trigonal space group $R32$ (D_3^7). The Er^{3+} ion is a popular active ion used in solid state lasers. For example, laser generation was obtained in the $YAl_3(BO_3)_4$ crystal with Er^{3+} ions as admixture [1–3]. The huntite-like structure has no center of inversion. Therefore, crystals of this type can be used as nonlinear active media as well [4,5]. $ErFe_3(BO_3)_4$ crystal, the same as a number of other ferroborates, undergoes the structural phase transition to the lower space symmetry $P3_121$ (D_3^4) with the temperature decrease. After this transition, the local symmetry of the RE ion decreases from D_3 to C_2 one. Deviation of the $ErFe_3(BO_3)_4$ space symmetry from the $R32$ one was so small that it was not identified by the X-ray diffraction measurements [6]. From the heat capacity measurements it was found out, that the first order structural phase transition to lower symmetry occurs in the $ErFe_3(BO_3)_4$ at 433–439 K [7]. Magnetic properties of the crystal are highly anisotropic [8,9], and temperature dependence of its paramagnetic magnetization deviates from the Curie-Weiss law.

A number of ferroborates of the $RFe_3(BO_3)_4$ type reveal multiferroic properties [10], that is, they have magnetic and electric polarizations simultaneously. However, the $ErFe_3(BO_3)_4$ crystal has very small electric polarization in magnetically ordered state [10] in contrast to the $ErAl_3(BO_3)_4$ crystal, which reveals rather large electric polarization in magnetic field [11]. Below 30–40 K all RE ferroborates are magnetically ordered. In particular, the $ErFe_3(BO_3)_4$ crystal becomes easy plane antiferromagnetic at $T_N = 38$ K [8,9,12].

Magnetic circular dichroism (MCD) of *f-f* transitions in solids is widely studied. We will mention only works devoted to the Er^{3+} ion. For example, the MCD was studied in the erbium containing glasses [13–16] and in the crystals [17,18]. The MCD can help to find the Zeeman splitting, when it is not resolved in the spectrum directly [19]. Additionally, the MCD can help to identify electronic states. The paramagnetic MCD of the parity forbidden *f-f* transitions gives also information about the nature of the *f-f* transitions allowance [19]. Temperature dependences of the integral paramagnetic magneto-optical activity (MOA) of *f-f* absorption bands in the $ErFe_3(BO_3)_4$ and $ErAl_3(BO_3)_4$ single crystals were measured and analyzed in Ref. [7].

The *f-f* transitions are partially allowed due to deviation of the local symmetry of a RE ion from the centrosymmetrical one. Therefore, properties of the *f-f* transitions are very sensitive to small local distortions. In the present work we studied spectra of absorption and MCD of *f-f* transitions in the $ErFe_3(BO_3)_4$ crystal and compared them with the corresponding spectra in the $ErAl_3(BO_3)_4$ crystal, which has the same structure, but higher local symmetry of the Er^{3+} ions. Indeed, we

---

* Corresponding author.
  E-mail address: malakha@iph.krasn.ru (A.V. Malakhovskii).

revealed substantial differences both in the absorption and MCD spectra of the discussed crystals.

2. Experimental details

ErFe$_3$(BO$_3$)$_4$ single crystals were grown from the melt solution as described in Ref. [9]. As grown-up crystals had the size of $5 \times 5 \times 7$ mm^3. As mentioned above, the ErFe$_3$(BO$_3$)$_4$ crystal belongs to the trigonal symmetry. The lattice constants of the ErFe$_3$(BO$_3$)$_4$ are [6]: $a = 9.566(4)$ Å, $c = 7.591(3)$ Å. The unit cell contains three formula units. At the temperature of the measurements (90 K) the crystal has $P3_121$ (D_3^4) space symmetry. All Er^{3+} ions are in positions of only one type. They are located in the center of trigonal prisms with the C_2 symmetry composed of six oxygen ions. The FeO$_6$ octahedrons form three mutually independent helicoidal chains, which run parallel to the C_3 axis.

As mentioned above, the Er^{3+} ions are located in the C_2 positions, however, the crystal as a whole remains the trigonal one. Correspondingly, absorption spectra were obtained for three polarizations: when the light propagated normally to the C_3 axis of the crystal 1) for the light electric vector $\overrightarrow{E}$ parallel (π polarization) and 2) perpendicular (σ polarization) to the C_3 axis and 3) for the light propagating along the C_3 axis (α polarization). Optical slit width (spectral resolution) was 0.2 nm in the region of 300–600 nm and 0.4 nm in the region of 600–1100 nm.

The MCD spectra were recorded with the light propagated along the trigonal axis of the crystal in the magnetic field of 5 kOe also directed along the C_3 axis. The circular dichroism was measured by the dichroism spectrometer described in Ref. [20] and based on modulation of the light wave polarization with the piezoelectric modulator. The MCD was obtained as a half difference of the circular dichroisms at opposite magnetic fields. Thus, the natural circular dichroism was excluded. The sensitivity in measuring of the circular dichroism was 10^{-4}, and the spectral resolution was the same as that at the absorption spectra measuring. The sample was put in a nitrogen gas flow cryostat. Accuracy of the temperature measuring was ~1 K. Thickness of the ErFe$_3$(BO$_3$)$_4$ samples was ~0.2 mm.

3. Results and discussion

Linearly polarized absorption and MCD spectra of the ErFe$_3$(BO$_3$)$_4$ were measured at $T = 90$ K for f-f absorption bands: $^4I_{15/2} \rightarrow {}^4I_{11/2}$ (A band), $^4I_{9/2}$ (B band), $^4F_{9/2}$ (D band), $^4S_{3/2}$ (E band), $^2H_{11/2}$ (F band) and $^4F_{7/2}$ (G band), (see Figs. 1–7). Identification of f-f absorption bands was made according to Kaminskii [21]. Within the limits of the experimental error the absorption spectra of the crystal in the σ and α polarizations coincide, that testifies to the electric dipole character of the transitions. Absorption spectrum of the ErFe$_3$(BO$_3$)$_4$ crystal (Fig. 1) consists of narrow bands corresponding to f-f transitions in Er^{3+} ions and of wide bands corresponding to d-d transitions in Fe^{3+} ions ($^6A_1 \rightarrow {}^4T_1$ and $^6A_1 \rightarrow {}^4T_2$ transitions in the cubic crystal field notation). At $E \sim 22900$ cm^{-1} a comparatively strong d-d transition $^6A_1 \rightarrow {}^4A_1{}^4E$ [22] observes. At $E \sim 25000$ cm^{-1} the strong absorption caused by the interatomic Fe-Fe (Mott-Hubbard) transitions begins. These transitions overlap the f-f transitions. The d-d absorption bands were approximated by the Gauss functions and subtracted from the total spectra. Thus, the f-f absorption spectra were obtained. MCD of the d-d transitions appeared to be too small to be observed (Fig. 1). The f-f absorption spectra of the ErFe$_3$(BO$_3$)$_4$ and also measured earlier absorption spectra of the ErAl$_3$(BO$_3$)$_4$ [23] were decomposed on components of the Lorentz shape and their intensities were determined (see Table 1).

In ErAl$_3$(BO$_3$)$_4$ all transitions, both from the lowest level and from the upper levels of the ground multiplet, were identified basing on their polarizations and the selection rules presented in Table 2 for the D_3 local symmetry [23]. In the C_2 local symmetry of the Er^{3+} ion in

ErFe$_3$(BO$_3$)$_4$ there is only one irreducible representation, $E_{1/2}$, for states with the half-integer moments, and consequently all transitions can have all polarizations. Therefore, identifying transitions in ErFe$_3$(BO$_3$)$_4$, we based on the comparison of the ErFe$_3$(BO$_3$)$_4$ absorption spectra with those of ErAl$_3$(BO$_3$)$_4$ [23]. The results are shown in Figs. 2–7 and Table 1. The capital letters indicate transitions from the ground state and the lower case characters indicate transitions from the upper states of the ground multiplet or vibronic transitions. The total splitting of the excited multiplets in the crystal field, found from the absorption spectra (Figs. 2–7), are shown in Table 3. The splitting of some excited states are appreciably different in ErFe$_3$(BO$_3$)$_4$ and in ErAl$_3$(BO$_3$)$_4$. This means that the crystal field is different not only in these crystals, but also in different electron states of the same crystal.

Transitions from the upper components of the ground multiplet permitted us to find position of these components (Table 1). They are close to those presented in Ref. [24]. It is necessary to emphasize that positions of the ground multiplet sublevels (Table 1) obtained from different transitions are appreciably different. Dispersions of these values are shown in Table 1 in brackets. From this fact, we can conclude that the electron transition have an influence on the local properties of the crystal not only in the excited state but also in the initial one. According to the perturbation theory, electron transitions occur as a result of mixing of initial and final states by the time-dependent perturbation caused by an electromagnetic wave. Therefore, during the electron transition, the initial state of the ion and its interaction with the environment also changes and can have an influence on the energy of the state. Manifestations of this phenomenon were earlier revealed also in Refs. [19,25].

If a single absorption line is split on two components in magnetic field directed along the light propagation, then MCD can be written in the form:

$$\Delta k = k_{m+}\varphi(\omega, \omega_0 + \Delta\omega_0) - k_{m-}\varphi(\omega, \omega_0 - \Delta\omega_0) \tag{1}$$

Here k_{m+} and k_{m-} are amplitudes of $(+)$ and $(-)$ circularly polarized absorption lines; φ are form functions of $(+)$ and $(-)$ polarized lines. If the Zeeman splitting $\Delta\omega_0$ is much less than the line width, then:

$$\Delta k = k_m c\varphi(\omega, \omega_0) + k_m \Delta\omega_0 \partial\varphi(\omega, \omega_0)/\partial\omega_0 \tag{2}$$

Here $k_m = k_{m+} + k_{m-}$ is the amplitude of the line not split by the magnetic field and $c = (k_{m+} - k_{m-})/k_m$. The first term in (2) is the paramagnetic MCD and the second one is the diamagnetic MCD. The Zeeman splitting $\Delta\omega_0$ is the measure of the diamagnetic MCD. The fine structure of the MCD spectra (Figs. 1–7) is due to the diamagnetic effect, but integral of the MCD spectrum over multiplet gives the integral paramagnetic MCD of the multiplet (the integral of the diamagnetic part is evidently zero). Temperature dependences of the integral paramagnetic MCD in ErFe$_3$(BO$_3$)$_4$ were studied in Ref. [7].

For the MCD written in the form (1), it is easy to show [19] that the diamagnetic effect $\Delta\omega_0$ is negative if signs of $\partial k/\partial\omega$ and $\Delta k(\omega)$ coincide, and vise versa. However, it is more convenient to find signs of $\Delta\omega_0$ comparing absorption (k) and $\partial\Delta k/\partial\omega$ spectra. Signs of extremums of the latter function at positions of absorption lines give signs of the diamagnetic effect [19]. Thus, we found signs of the diamagnetic effects of the f-f transitions from the experimental MCD spectra (Figs. 2–7, Table 1). If absorption and MCD spectra of a transition are spectrally good resolved, it is possible to find the value of the Zeeman splitting $\Delta\omega_0$, using the absorption and MCD spectra. For the absorption line of the Lorentz shape (as in our case) it is [19]:

$$\Delta\omega_0 = 2\frac{\Delta k_{dm}}{k_m}|\omega_m - \omega_0| \tag{3}$$

Here Δk_{dm} and ω_m are the value and position of extremums of the diamagnetic MCD of the line, respectively, and k_m is amplitude of the α-absorption of the line. The splitting of the Kramers doublets in magnetic field H directed along the C_3 axis of a crystal is given in the form: $\Delta E = \mu_B g_C H$, where g_C is the effective Landé factor in the C_3-direction.
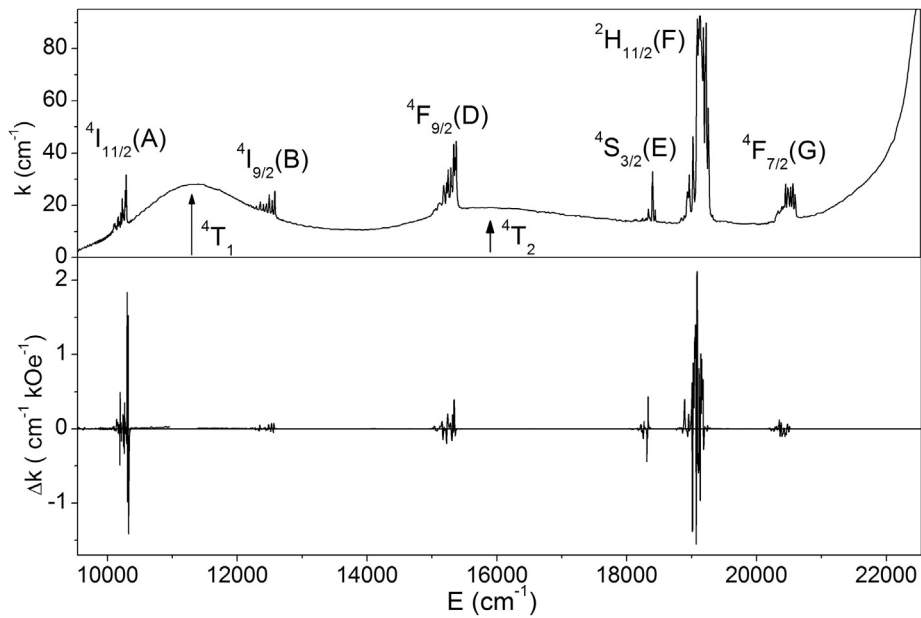
Fig. 1. α-polarized absorption spectra (k) and MCD spectra (Δk) of ErFe$_3$(BO$_3$)$_4$ at 90 K.

Therefore, for the transitions between the Kramers doublets

$$2\hbar\Delta\omega_0 = \mu_B H \Delta g_C \qquad (4)$$

Here Δg_C is the difference of the effective Landé factors g_C of states taking part in the transition. These values were found for the good resolved lines (see Table 1). Signs of Δg_C correspond to signs of $\Delta\omega_0$. The purely π-polarized lines have, evidently, no MCD.

In the axial crystals the electron states can be described in a first approximation by $|J, \pm M_J\rangle$ wave functions of the free atom, where J and M_J are the total moment and its projection respectively. In this approximation it is possible to find the Landé factors of the Kramers doublets along the C_3 axis, g_{CM}, theoretically. They are evidently equal to: $g_{CM} = 2gM_J$ where g is the Landé factor of the free atom.

Corresponding values of Δg_{CM} were found in Ref. [23] (see Table 1) for some transitions in ErAl$_3$(BO$_3$)$_4$, for which values of M_J could be identified. This approximation cannot be strictly applied to the ErFe$_3$(BO$_3$)$_4$ crystal, since the local symmetry of the Er^{3+} ion in this crystal is C_2. However, found values of Δg_{CM} can be used as some guideline, since the ErFe$_3$(BO$_3$)$_4$ crystal as a whole has trigonal symmetry. Just due to this circumstance it was possible to measure MCD. All obtained characteristics of the transitions are presented in Table 1 in detail. However, we shall pay attention on some features in all absorption bands.
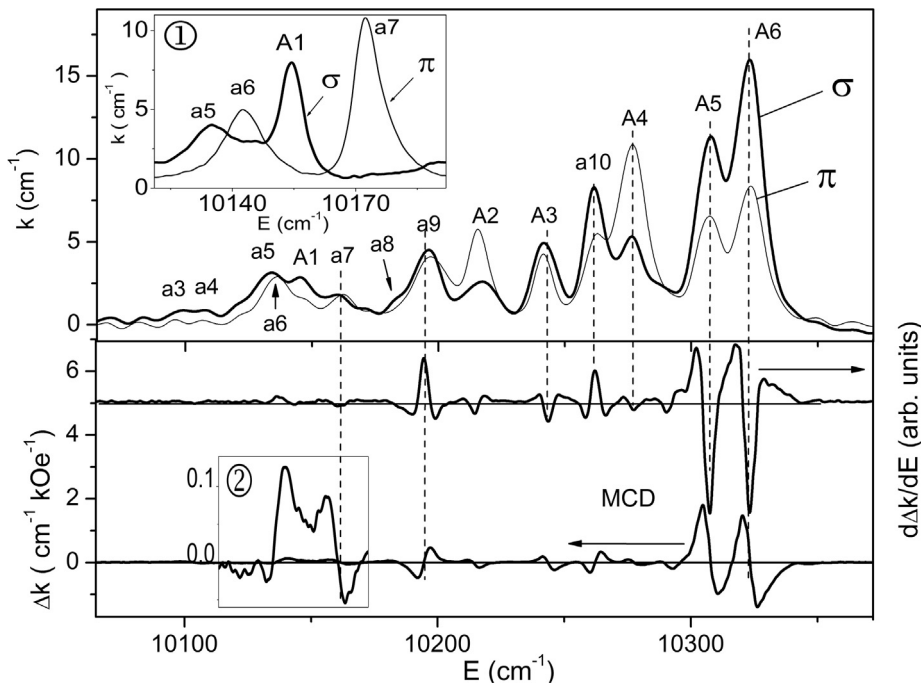

Fig. 2. Absorption (k), MCD (Δk) and derivative of the MCD ($d\Delta k/dE$) spectra of $^4I_{15/2} \rightarrow {}^4I_{11/2}$ transition (A band) at 90 K. Inset (1) shows absorption of ErAl$_3$(BO$_3$)$_4$. Inset (2) shows MCD spectrum of lines a5, A1 and a7 in ErFe$_3$(BO$_3$)$_4$ in the increased scale.
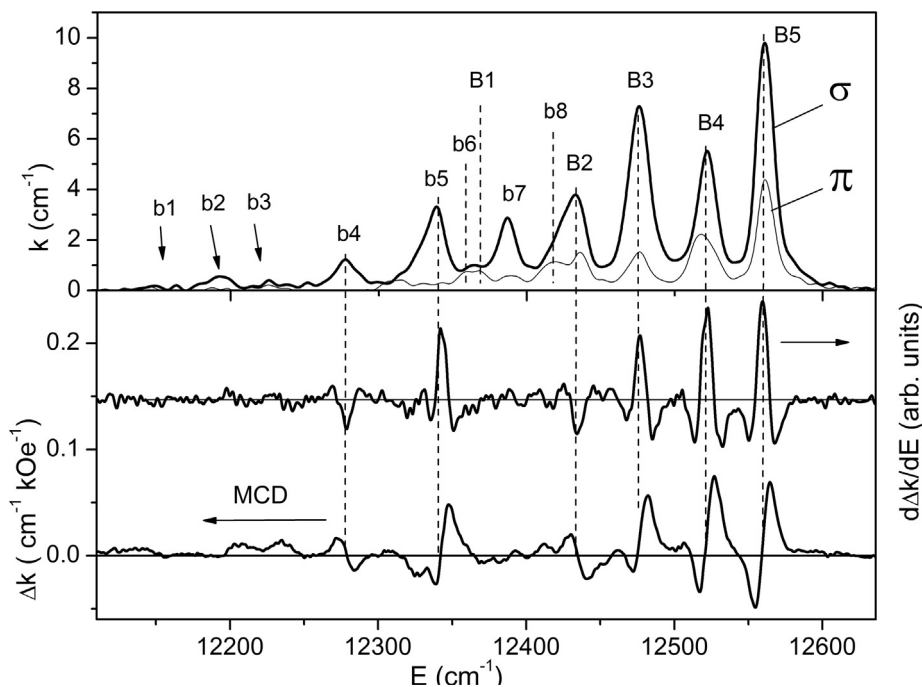
Fig. 3. Absorption (k), MCD (Δk) and derivative of the MCD (dΔk/dE) spectra of $^4I_{15/2} \rightarrow {}^4I_{9/2}$ transition (B band) at 90 K.

3.1. Transition $^4I_{15/2} \rightarrow {}^4I_{11/2}$ (A band)

A1 and A2 lines, being σ-polarized in ErAl₃(BO₃)₄, appeared in ErFe₃(BO₃)₄ in π-polarization, however intensity of the A1 line in σ-polarization strongly decreased (Table 1). Strong in ErAl₃(BO₃)₄ π-polarized line a7, identified as vibrational repetition of the transition from the Gr4 level, strongly decreased in ErFe₃(BO₃)₄ but became πσ polarized (Fig. 2, inset 1) and, correspondingly, the MCD appeared (Fig. 2, inset 2, Table 1). Signs of the Δg_C of transitions A3 and a9 in Er-Fe₃(BO₃)₄ are opposite to those in ErAl₃(BO₃)₄ (Table 1).

3.2. Transition $^4I_{15/2} \rightarrow {}^4I_{9/2}$ (B band)

B2 and B4 lines appeared in ErFe₃(BO₃)₄ in π-polarization, but their intensity in σ-polarization substantially decreased (Fig. 3, Table 1). Signs of Δg_C of transitions B2, B3 in ErFe₃(BO₃)₄ are opposite to those in ErAl₃(BO₃)₄, while in ErAl₃(BO₃)₄ the experimental and theoretical values are close to each other (Table 1). Value of Δg_C of the b4 transition is close to the theoretical one for ErAl₃(BO₃)₄ (Table 1).
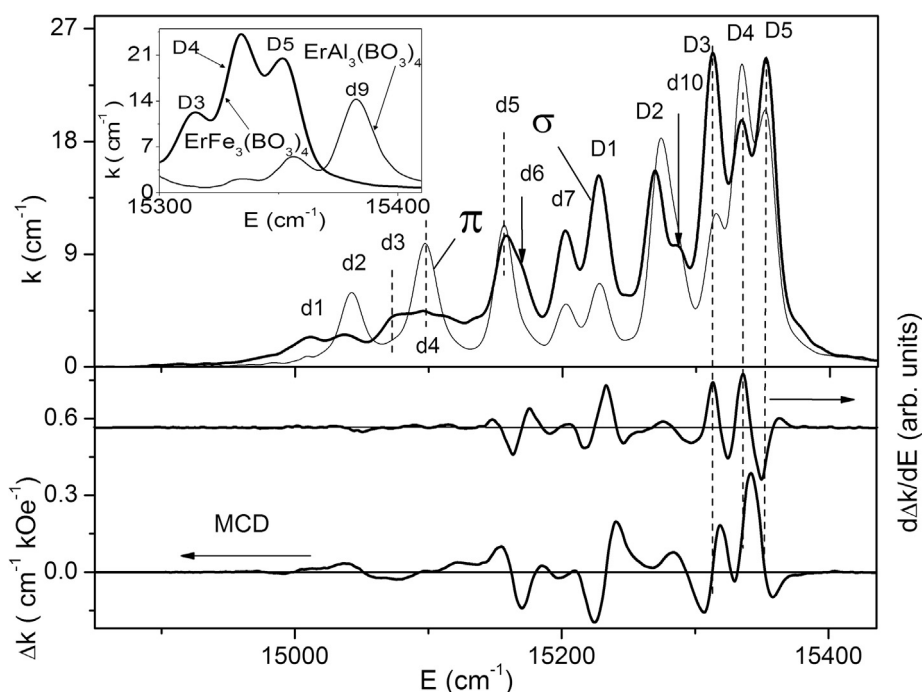

Fig. 4. Absorption (k), MCD (Δk) and derivative of the MCD (dΔk/dE) spectra of $^4I_{15/2} \rightarrow {}^4F_{9/2}$ transition (D band) at 90 K. Inset shows comparison of ErAl₃(BO₃)₄ and ErFe₃(BO₃)₄ π-polarized absorption spectra.

Fig. 5. Absorption (k), MCD (Δk) and derivative of the MCD ($d\Delta k/dE$) spectra of $^4I_{15/2} \rightarrow {}^4S_{3/2}$ transition (E band) at 90 K.

3.3. Transition $^4I_{15/2} \rightarrow {}^4F_{7/2}$ (G band)

Transition G4 was very weak in ErAl$_3$(BO$_3$)$_4$ (Table 1). In Er-Fe$_3$(BO$_3$)$_4$ it is not observed at all (Fig. 7). Transitions g1 and g2 from excited levels are also much weaker in ErFe$_3$(BO$_3$)$_4$ (Table 1).

3.4. Transition $^4I_{15/2} \rightarrow {}^4S_{3/2}$ (E band)

E2 and e2 lines appeared in π-polarization and e3 line appeared in σ-polarization in ErFe$_3$(BO$_3$)$_4$ (Fig. 5, Table 1). Intensity of the vibronic

line e4, being the vibrational repetition of the E1 transition, strongly increased in ErFe$_3$(BO$_3$)$_4$ as compared with ErAl$_3$(BO$_3$)$_4$ (Table 1). This line gives energy 103 cm^{-1} of one of the local vibrations in the excited E1 state. This value is close to 109 cm^{-1} found from the optical spectra of ErAl$_3$(BO$_3$)$_4$ [23], but rather far from that found in ErFe$_3$(BO$_3$)$_4$ [26] from the Raman scattering measurements: 181 and 84 cm^{-1}. The cause of such discrepancy is that the Raman scattering studies collective vibrations (phonons) of the crystal in the ground electron state, while the optical absorption measurements give local vibrations in the optically excited states.
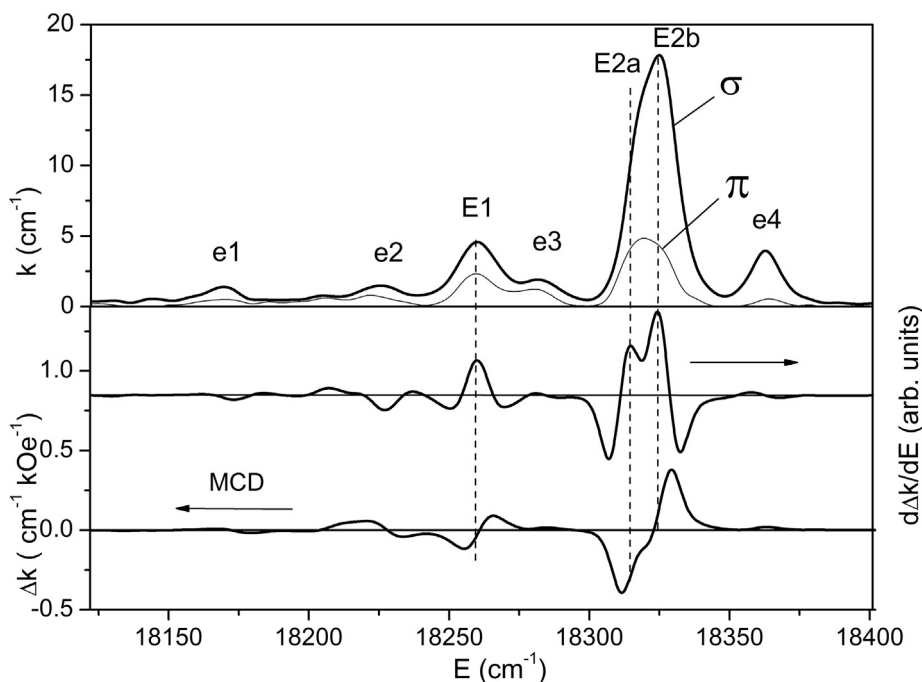

Fig. 6. Absorption (k), MCD (Δk) and derivative of the MCD ($d\Delta k/dE$) spectra of $^4I_{15/2} \rightarrow {}^2H_{11/2}$ transition (F band) at 90 K. Inset shows comparison of ErAl$_3$(BO$_3$)$_4$ and ErFe$_3$(BO$_3$)$_4$ π- and σ-polarized absorption spectra in the region of f10 and f11 lines.
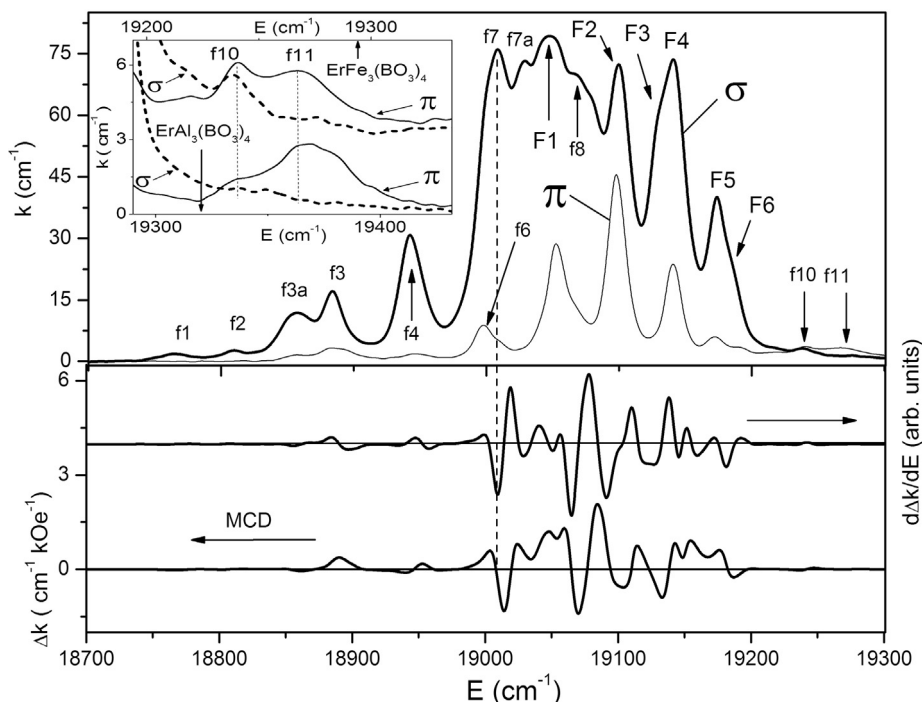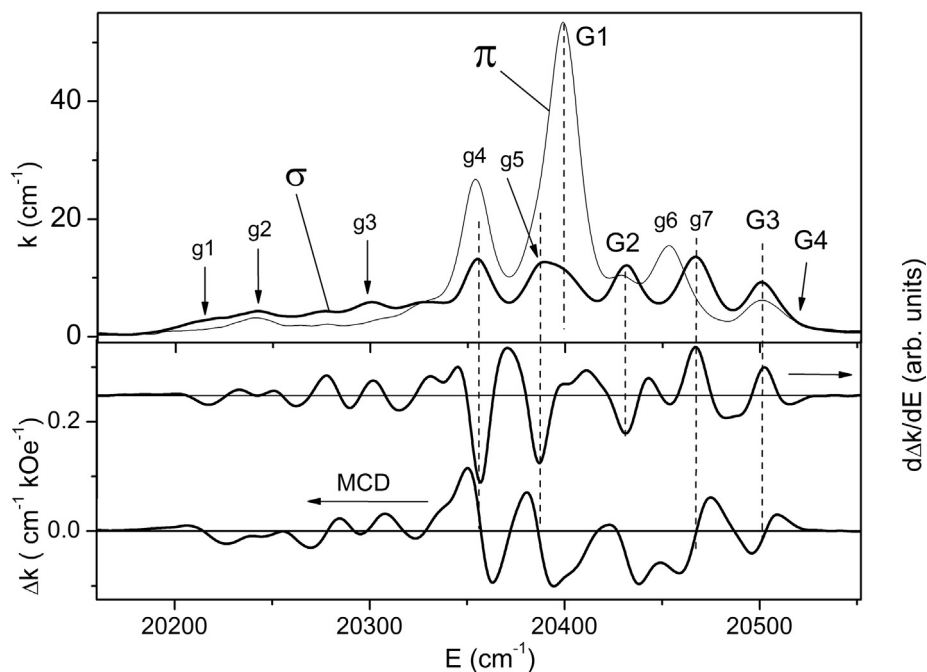
Fig. 7. Absorption (k), MCD (Δk) and derivative of the MCD ($d\Delta k/dE$) spectra of $^4I_{15/2} \rightarrow {}^4F_{7/2}$ transition (G band) at 90 K.

A splitting of the E2 line in ErAl$_3$(BO$_3$)$_4$ was very small (< 5 cm^{-1}) and was found only in the natural circular dichroism spectrum [27]. In ErFe$_3$(BO$_3$)$_4$ this splitting is much larger (10 cm^{-1}) and is seen directly on the absorption and MCD spectra (Fig. 5). The splitting of the Kramers doublets is impossible in CF of any symmetry. We refer this splitting to the existing of two kinds of absorbing centers. The discussed splitting is observed only on one transition. Consequently, this phenomenon occurs only in the definite excited state and has the local character. In the huntite structure with $R32$ space symmetry the rare earth ions occupy three equivalent positions with the D_3 local symmetry in the unit cell. At the lower space symmetry $P3_121$ the local symmetry of the rare earth ions decreases to C_2 one, but positions remain equivalent. However it is known, that the unit cell of the huntite structure can have also the $C2$ space symmetry [28]. In a number of alumoborates such modification of the crystals was revealed experimentally in the ground electron state [29]. The unit cell of the huntite structure in the $C2$ space symmetry is twice as large and it has four RE ions in C_1 symmetry positions and two RE ions in C_2 symmetry positions. Of course, the local distortions in the excited state do not strictly correspond to the $C2$ symmetry, but can be similar to it.

3.5. Transition $^4I_{15/2} \rightarrow {}^2H_{11/2}$ (F band)

Additional line f3a (Fig. 6), which can be referred to the transition Gr6 → F2, appeared, but f5 line disappeared as compared with ErAl$_3$(BO$_3$)$_4$ (Table 1). F4 line appeared in π-polarization. Additional line f7a was resolved. It can be referred to the transition Gr4 → F5. Line f10 was observed in ErAl$_3$(BO$_3$)$_4$ only in π-polarization, but in ErFe$_3$(BO$_3$)$_4$ it is πσ-polarized (Table 1, Fig. 6, inset). Energies of lines f10 and f11 are larger than energies of all transitions from the ground state. This is possible only if the lines correspond to electron-vibrational (vibronic) transitions. Purely π-polarization of these lines in ErAl$_3$(BO$_3$)$_4$ indicated, according to the selection rules from Table 2, that the transitions occurred not from the ground state E$_{1/2}$. We supposed that f10 and f11 lines are vibrational repetitions of the transitions Gr2 → F5 and Gr2 → F6. Then we obtain energies of vibrations 115 and 121 cm^{-1}, respectively (Table 1). The existence of the discussed lines would be not surprising, if these lines were not so strong in contrast to the usual f-f vibronic transitions from the ground state. (Compare

intensities of the discussed lines (Table 1) with those of the e4 line especially in ErAl$_3$(BO$_3$)$_4$.) Additionally, the purely electron origins of these vibronic transitions are not observed. This situation resembles that occurred for the d-d transitions in 3d compounds, when practically only vibronic transitions allowed by odd vibrations are observed. Weak vibronic f-f transitions occur from the ground state while the discussed ones - from the excited states. Thus, the intensive vibronic transitions occur between two excited states and we can suppose that the local environment of the Er^{3+} ion in these excited states is close to the centrosymmetrical one and that the electron-vibrational interaction with the odd vibrations, which allows the f-f transitions, takes place and is strong. In addition, it is worth noting that energies of the same vibrations, found from vibronic transitions f10, f11 and e4, are appreciably different (see Table 1). It happens so, since we deal with the local vibrations in different excited states.

3.6. Transition $^4I_{15/2} \rightarrow {}^4F_{9/2}$ (D band)

d4, d7, D1 and D3 lines (Fig. 4) appeared in π-polarization and D4 and D5 lines strongly increased in π-polarization in ErFe$_3$(BO$_3$)$_4$ as compared width ErAl$_3$(BO$_3$)$_4$ (Table 1). A new line d10 appeared. It is possible to suppose that this line is due to the transition Gr2 → D4 from the excited level Gr2 (48 cm^{-1}) of the ground multiplet. Purely π-polarized in ErAl$_3$(BO$_3$)$_4$ line d5 (Table 1) became πσ polarized in ErFe$_3$(BO$_3$)$_4$ (Fig. 4, Table 1). Correspondingly, this transition revealed some MCD (Fig. 4, Table 1).

π-polarized lines d8 (Table 1) and d9 (Fig. 4 inset, Table 1) observed in ErAl$_3$(BO$_3$)$_4$ disappeared in ErFe$_3$(BO$_3$)$_4$. As mentioned above, π-polarization in ErAl$_3$(BO$_3$)$_4$ means that the transition occurs not from the ground state. Additionally, transition d9 is certainly vibronic one similar to the f10 and f11 transitions. Intensity of transitions f10 and f11 is of the same order of magnitude in ErFe$_3$(BO$_3$)$_4$ and ErAl$_3$(BO$_3$)$_4$. On the contrary, the d9 transition has the extraordinary large pure π-polarized intensity in ErAl$_3$(BO$_3$)$_4$ (Fig. 4, inset, Table 1), but totally disappears in ErFe$_3$(BO$_3$)$_4$. Therefore, we can conclude that, in contrast to ErAl$_3$(BO$_3$)$_4$, local environment of the Er^{3+} ion in ErFe$_3$(BO$_3$)$_4$ in the initial and final states of the transition d9 is substantially non centrosymmetric, and allowance of f-f transitions by odd vibrations occurred in ErAl$_3$(BO$_3$)$_4$ is substituted by static odd distortions.

Table 1

Energies of states (E), experimental changes of the Landé factors along the C_3 axis during transitions (Δg_C) and the same values found theoretically in the $|J, \pm M_J\rangle$ function approximation for ErAl$_3$(BO$_3$)$_4$ (Δg_{CM}).

Multiplets	Levels (Transitions)	E (cm^{-1}) ErAl$_3$(BO$_3$)$_4$ [27]	E (cm^{-1}) ErFe$_3$(BO$_3$)$_4$	Intensity (cm^{-2})				Δg_C		Δg_{CM} [27]
				ErAl$_3$(BO$_3$)$_4$		ErFe$_3$(BO$_3$)$_4$		ErAl$_3$(BO$_3$)$_4$[27]	ErFe$_3$(BO$_3$)$_4$	
				π	σ	π	σ			
$^4I_{15/2}$	Gr1	0	0							
	Gr2	46	44 (35–47)							
	Gr3	104	106 (91–114)							
	Gr4	122	139 (127–147)							
	Gr5	160	178 (175–182)							
	Gr6	233	231 (221–242)							
	Gr7	263	267 (259–275)							
	Gr8	293	297							
$^4I_{11/2}$(A)	A1	10,153	10,146	no	120	10.4	26.3	(−)		
	A2	10,207	10,215	no	36	60.3	47.8	(−)	−7.12	
	A3	10,220	10,242	2.43	111	37.4	73.9	(+)	(−)	
	A4	10,252	10,276	116	106	201	80	(−)	−2.51	
	A5	10,290	10,307	76.2	220	70.4	172	(−)	−19.7	
	A6	10,299	10,323	89.8	259	138	317	(−)	−14.5	
	a1(Gr6 → A6)	10,061	no	25.9	30	no	no			
	a2(Gr4 → A2)	10,091	no	81.7	no	no	no	no		no
	a3(Gr4 → A3)	10,098	10,096	no	146	small	small	(−)?		
	a4(Gr3 → A2)	10,113	10,109	no	24	small	small			
	a5(Gr4 → A4)	10,135	10,134	no	134	no	93.2	(−)	(+)	
	a6(Gr3 → A4)	10,142	no	89.5	no	46.6	no			
	a7(Gr4 → A2 + 84(A$_2$))	10,172	10,162	130	no	19.4	30	no	−12.4	no
	a8	10,190	10,182	no	9.95	no	12.7			
	a9(Gr3 → A6)	10,201	10,197	18.3	62.9	93.5	83.3	(−)	+14.7	
	a10(Gr2 → A5)	10,244	10,261	no	45.6	43.8	118	(+)	(+)	
$^4I_{9/2}$(B)	B1	12,396	12,363	26.3	12.1	25.3	8.9			(−)
	B2	12,444	12,433	no	174	20.7	47.5	+11.3	(−)	+13.4
	B3	12,483	12,475	92.2	36.7	28.3	160	−10.8	+2.88	−12
	B4	12,534	12,522	no	163	61	108	+7.33	+3.67	+9.06
	B5	12,564	12,561	99.3	125	77.3	188	(+)	+2.13	(−)
	b1(Gr6 → B3)	12,253	no	4.35	23.5	no	no	−20.2		−4.76
	b2(Gr8 → B5)	12,283	12,191	31.2	21.4	no	15.6			
	b3(Gr6 → B4)	12,300	no	no	20	no	no			
	b4(Gr5 → B3)	12,323	12,277	no	28	no	28.6	−22.3	−5.89	−7.23
	b5(Gr4 → B3)	12,364	12,339	no	192	no	65.1	+10.6	+4.6	−14.4
	b6(Gr3 → B3)	12,375	12,359	38.1	no	no		(−)		
	b7(Gr5 → B5)	12,407	12,386	no	48.7	6.1	53.1			
	b8(Gr4 → B5)	no	12,414	no	small	31.1	49.7			
$^4F_{9/2}$(D)	D1	15,231	15,226	no	600	153	402		+13.5	
	D2	15,279	15,269	498	151	210	380		(+)	
	D3	15,313	15,314	no	293	224	577		+2.94	
	D4	15,337	15,333	15.8	491	344	350	(−)	(+)	
	D5	15,357	15,352	75.6	392	399	616	(−)	−2.36	
	d1(Gr7 → D1)	14,964	15,010	no	6.09	14	61			
	d2(Gr6 → D2)	15,040	15,042	173	108	157	35.2			
	d3	15,090	15,076	23.3	26.8	no	42.5			
	d4(Gr3 → D1)	15,119	15,096	no	106	272	350			
	d5(Gr5 → D3)	15,147	15,155	260	no	240	230	no	−9.42	no
	d6(Gr5 → D4)	15,173	15,170	no	141	no	103			
	d7(Gr3 → D3)	15,198	15,202	no	464	99.6	206			
	d8	15,218	no	90.2	no	no	no	no	no	no
	d9	15,383	no	396	no	no	no	no	no	no
	d10(Gr2 → D4)		15,285	no	no	277	86.8			
$^4S_{3/2}$ (E)	E1	18,322	18,260	18.6	197	36.1	66		+10.1	−17.6
	E2a	18,380	18,315	no	198	39.8	114	+7.14	+11.5	+9.6
	E2b	18,385	18,325	no	198	56.3	232		+6.9	
	e1(Gr3 → E1)	18,224	18,169	38.7	16.2	11.8	13.1	+7.38	−11.3	+11.2
	e2(Gr2 → E1)	18,274	18,225	no	75.4	12.1	17.8	−8.33	(−)	−16
	e3(Gr2 → E2)	18,332	18,283	35.1	no	22.3	21.6	no		
	e4 (E1 + 103)	18,429	18,363	12.8	8.4	6.22	49.1			

Table 1 (continued)

Multiplets	Levels (Transitions)	E (cm⁻¹) ErAl₃(BO₃)₄ [27]	E (cm⁻¹) ErFe₃(BO₃)₄	Intensity (cm⁻²)				Δg$_C$		Δg$_{CM}$ [27]
				ErAl₃(BO₃)₄		ErFe₃(BO₃)₄		ErAl₃(BO₃)₄[27]	ErFe₃(BO₃)₄	
				π	σ	π	σ			
²H₁₁/₂(F)	F1	19,138	19,047	197	3721	576	2911			
	F2	19,174	19,100	245	709	1018	1198	(+)		
	F3	19,224	19,132	no	1008	no	657		(−)	
	F4	19,236	19,140	no	1605	439	1632		(+)	
	F5	19,267	19,172	20.7	198	89.9	741	(−)	(+)	
	F6	19,282	19,193	69.1	380	62.6	102	(−)	(−)	
	f1	18,828	18,763	no	91.3	no	40.3	(+)		
	f2	18,853	18,811	no	94.4	no	30.3	(+)		
	f3a	no	18,858	no	no	17.6	436		(−)	
	f3	18,969	18,884	85.3	781	135	367	(−)	(+)	
	f4(Gr3 → F1)	19,019	18,942	79.2	612	33.3	926	+7.27	(+)	
	f5(Gr5 → F3)	19,065	no	114	no	no	no	no	no	no
	f6(Gr5 → F4)	19,081	18,998	163	no	209	no	no		
	f7(Gr2 → F1)	19,092	19,008	no	964	no	2189	(−)	(−)	
	f7a(Gr4 → F5)	no	19,028	no	no	no	1009			
	f8(Gr3 → F5)	19,159	19,070	183	289	194	2456	(−)		
	f9(Gr2 → F4)	19,187	no	498	no	no	no	no		
	f10(Gr2 → F5 + 115)	19,335	19,241	16	no	65	22.8		(+)	
	f11(Gr2 → F6 + 121)	19,370	19,268	150	no	175	no	no		
⁴F₇/₂(G)	G1	20,481	20,399	1137	344	1568	213			
	G2	20,509	20,431	184	217	48.6	254	(−)	(−)	
	G3	20,597	20,500	no	361	144	220	(−)	+2.1	
	G4	20,615	~20510	40.1	8.34					
	g1(Gr8 → G4)	20,328	20,219	6.72	253	6.22	51.8	(−)		
	g2(Gr7 → G4)	20,352	20,241	227	270	108	149	(−)		
	g3(Gr3 → G1)	20,403	20,301	23.6	201	28.7	178	(−)		
	g4(Gr3 → G2)	20,436	20,355	153	359	618	286	(+)	−8.58	
	g5(Gr2 → G2)	20,463	20,387	no	291	no	229	(−)	−5.9	
	g6(Gr2 → G3)	20,548	20,453	580	no	405	no	no		
	g7(Gr2 → G4)	20,571	20,467	no	244	no	357	+1.8	+3.43	

Table 2
Selection rules for electric dipole transitions in D_3 symmetry.

	$E_{1/2}$	$E_{3/2}$
$E_{1/2}$	π, σ(α)	σ(α)
$E_{3/2}$	σ(α)	π

Table 3
Splitting (ΔE) of the excited multiplets in the crystal field.

Symbol	Excited state	ΔE (cm⁻¹)	
		ErAl₃(BO₃)₄ [27]	ErFe₃(BO₃)₄
A	⁴I₁₁/₂	146	177
B	⁴I₉/₂	168	198
D	⁴F₉/₂	126	126
E	⁴S₃/₂	63	65
F	²H₁₁/₂	144	146
G	⁴F₇/₂	134	111

4. Summary

Linearly polarized absorption and MCD spectra of ErFe₃(BO₃)₄ single crystal were measured in the range of 9000–23000 cm⁻¹ at 90 K. The absorption spectra of *f-f* transitions were decomposed into the Lorentz shape components and intensities of the components were found. Positions of the ground multiplet levels obtained from the different transitions are appreciably different. This means that the electron transition have an influence on the local properties of the crystal not only in the excited state but also in the initial one. The total splitting of some excited multiplets in the crystal field are appreciably different in ErFe₃(BO₃)₄ and in ErAl₃(BO₃)₄. This means that the crystal field is different not only in these crystals, but also in different electron states of the same crystal. The MCD spectra permitted us to measure the Zeeman splitting of some transitions and so to determine changes of the Landé factor along the C_3 axis of the crystal during these transitions. Optical and magneto-optical properties of *f-f* transitions in the ErFe₃(BO₃)₄ crystal were compared with those in the ErAl₃(BO₃)₄ crystal with the higher local symmetry of the Er³⁺ ion. In particular, the pronounced changes of the transitions polarization, intensity and the Zeeman splitting (including its sign) occurred. Intensive *f-f* vibronic transitions, corresponding to the electron transitions from the upper components of the ground multiplet, were revealed. Large splitting of one of the *f-f* transitions, which is not possible for the Kramers doublets, was found out. It was explained by appearance of two absorbing centers in the excited state due to the local decrease of the symmetry in the excite state. In particular, this can be the local change of the space symmetry $P3_121$ to the structure similar to the $C2$ space group. In the unit cell of this structure there are two non equivalent positions of the Er³⁺ ion. Appreciable difference of the local vibrations energies in excited states ⁴S₃/₂ and ²H₁₁/₂ was revealed.

References

[1] Y.J. Chen, Y.F. Lin, X.H. Gong, Q.G. Tan, Z.D. Luo, Y.D. Huang, 2.0 W diode-pumped Er:Yb:YAl₃(BO₃)₄ laser at 1.5-1.6 μm, Appl. Phys. Lett. 89 (2006) 241111–241113.
[2] N.I. Leonyuk, V.V. Maltsev, E.A. Volkova, O.V. Pilipenko, E.V. Koporulina,

V.E. Kisel, N.A. Tolstik, S.V. Kurilchik, N.V. Kuleshov, Crystal growth and laser properties of new RAl$_3$(BO$_3$)$_4$ (R = Yb, Er) crystals, Opt. Mater. 30 (2007) 161–163.

[3] Y. Chen, Y. Lin, X. Gong, J. Huang, Z. Luo, Y. Huang, Acousto-optic Q-switched self-frequency-doubling Er: Yb: YAl$_3$(BO$_3$)$_4$ laser at 800 nm, Opt. Lett. 37 (2012) 1565–1567.

[4] P. Dekker, J.M. Dawes, J.A. Piper, Y.G. Liu, J.Y. Wang, 1.1 W CW self-frequency-doubled diode-pumped Yb:YAl$_3$(BO$_3$)$_4$ laser, Opt. Commun. 195 (2001) 431–436.

[5] E. Cavalli, A. Speghini, M. Bettinelli, M.O. Ramirez, J.J. Romero, L.E. Bausa, J.G. Sole, Luminescence of trivalent rare earth ions in the yttrium aluminium borate non-linear laser crystal, J. Lumin. 102 (2003) 216–219.

[6] A.V. Malakhovskii, V.V. Sokolov, A.L. Sukhachev, A.S. Aleksandrovsky, I.A. Gudim, M.S. Molokeev, Spectroscopic properties and structure of the ErFe$_3$(BO$_3$)$_4$ single crystal, Phys. Solid State 56 (2014) 2056–2063.

[7] A.V. Malakhovskii, A.L. Sukhachev, V.V. Sokolov, T.V. Kutsak, V.S. Bondarev, I.A. Gudim, Magneto-optical activity of *f-f* transitions in ErFe$_3$(BO$_3$)$_4$ and ErAl$_3$(BO$_3$)$_4$ single crystals, J. Magn. Magn. Mater. 384 (2015) 255–265.

[8] E.A. Popova, A.N. Vasiliev, V.L. Temerov, L.N. Bezmaternykh, N. Tristan, R. Klingeler, B. Büchner, Magnetic and specific heat properties of YF$_e$(BO$_3$)$_4$ and ErF$_e$(BO$_3$)$_4$, J. Phys.: Condens. Matter. 22 (2010) 116006–116013.

[9] C. Ritter, A. Vorotynov, A. Pankrats, G. Petrakovskiĭ, V. Temerov, I. Gudim, R. Szymczak, Magnetic structure in iron borates RFe$_3$(BO$_3$)$_4$ (R = Er, Pr): a neutron diffraction and magnetization study, J. Phys.: Condens. Matter. 22 (2010) 206002–220609.

[10] A.M. Kadomtseva, Y.F. Popov, G.P. Vorob'ev, A.P. Pyatakov, S.S. Krotov, K.I. Kamilov, L.N. Bezmaternykh, Magnetoelectric and magnetoelastic properties of rare-earth ferroborates, Low Temp. Phys. 36 (2010) 511–521.

[11] K.-C. Liang, R.P. Chaudhury, B. Lorenz, Y.Y. Sun, L.N. Bezmaternykh, I.A. Gudim, V.L. Temerov, C.W. Chu, Magnetoelectricity in the system RAl$_3$(BO$_3$)$_4$ (R = Tb, Ho, Er, Tm), J. Physics: Conf. Series 400 (2012) 032046–032051.

[12] M.N. Popova, E.P. Chukalina, T.N. Stanislavchuk, L.N. Bezmaternykh, Different types of magnetic ordering in RFe$_3$(BO$_3$)$_4$, R = Gd, Tb, Er, and Y, as studied by the method of Er^{3+} spectroscopic probe, J. Magn. Magn. Mater. 300 (2006) e440–e443.

[13] S.J. Collocott, K.N.R. Taylor, Magneto-optical properties of erbium-doped soda glass, J. Phys. C: Solid State Phys. 11 (1978) 2885–2893.

[14] U.V. Valiev, A.A. Klochkov, A.S. Moskvin, P. Shiroki, Magnetooptics of 4f–4f for-bidden transitions in Er-3+-doped phosphate-glasses, Opt. Spektrosk. 69 (1990) 111–114.

[15] A.A. Klochkov, U.V. Valiev, A.S. Moskvin, The Role of 4f–4f transitions in magne-tooptics of paramagnetic rare-earth glasses, Phys. Status Solidi B 167 (1991) 337–348.

[16] D.P. Poulios, D.E. Johnson, N.P. Bigelow, J.P. Spoonhower, Methods of studying magnetic circular dichroism in erbium-doped aluminosilicate glass, J. Non-Cryst. Solids 239 (1998) 181–186.

[17] P.G. Feldmann, H. Le Gall, M. Guillot, Magnetic circular dichroism in erbium Iron garnet, IEEE Trans. Magn. (1985) 1669–1671 MAG-21.

[18] G. Corradi, Th. Lingner, A.B. Kutsenko, V. Dierolf, K. Polgar, J.-M. Spaeth, W. Von der Osten, Magneto-optical studies of Er^{3+} in stoichiometric LiNbO$_3$, Radiat. Erects Defects Solids 155 (2001) 223–227.

[19] A.V. Malakhovskii, A.L. Sukhachev, A.Yu. Strokova, I.A. Gudim, Magneto-optical activity of $f-f$ transitions and properties of 4f states in single-crystal DyF$_e$3(B$_O$3)4, Phys. Rev. B 88 (2013) 075103–075116.

[20] A.V. Malakhovskii, S.L. Gnatchenko, I.S. Kachur, V.G. Piryatinskaya, A.L. Sukhachev, I.A. Gudim, Optical and magneto-optical properties of Nd$_{0.5}$Gd$_{0.5}$Fe$_3$(BO$_3$)$_4$ single crystal in the near IR spectral region, J. Alloys Comp. 542 (2012) 157–163.

[21] A.A. Kaminskii, Crystalline Lasers: Physical processes and Operating Schemes, CRC Press, New York, London, Tokyo, 1996.

[22] A.V. Malakhovskii, A.L. Sukhachev, A.D. Vasil'ev, A.A. Leont'ev, A.V. Kartashev, V.L. Temerov, I.A. Gudim, Nature of optical properties of GdFe$_3$(BO$_3$)$_4$ and GdFe$_{2.1}$Ga$_{0.9}$(BO$_3$)$_4$ crystals and other 3d^5 antiferromagnets, Eur. Phys. J. B 85 (2012) 80.

[23] A.V. Malakhovskii, V.V. Sokolov, I.A. Gudim, Optical and magneto-optical spectra and electron structure of ErAl$_3$(BO$_3$)$_4$ single crystal, J. Alloys Compd. 698 (2017) 364–374.

[24] E.P. Chukalina, T.N. Stanislavchuk, M.N. Popova, B.Z. Malkin, L.N. Bezmaternykh, I.A. Gudim, in: Proceedings of the XXI International Conference "New in Magnetism and Magnetic Materials" (NMMM), Moscow, Russia, June 28–July 4, 2009 (Moscow, 2009), pp. 510–511.

[25] A.V. Malakhovskii, S.L. Gnatchenko, I.S. Kachur, V.G. Piryatinskaya, A.L. Sukhachev, V.L. Temerov, Magneto-optical spectra and electron structure of Nd$_{0.5}$Gd$_{0.5}$Fe$_3$(BO$_3$)$_4$ single crystal, J. Mag. Magn. Mater. 401 (2016) 517–524.

[26] D. Fausti, A.A. Nugroho, P.H.M. van Loosdrecht, S.A. Klimin, M.N. Popova, L.N. Bezmaternykh, Raman scattering from phonons and magnons in RFe$_3$(BO$_3$)$_4$, Phys. Rev. B 74 (2006) 024403.

[27] A.V. Malakhovskii, V.V. Sokolov, I.A. Gudim, Natural optical activity of f-f transi-tions in ErAl$_3$(BO$_3$)$_4$ single crystal, Chem. Phys. 493 (2017) 102–110.

[28] B.J. Campbell, H.T. Stokes, D.E. Tanner, D.M. Hatch, ISODISPLACE: a web-based tool for exploring structural distortions, J. Appl. Crystallogr. 39 (2006) 607–614.

[29] P.A. Plachinda, E.L. Belokoneva, High temperature synthesis and crystal structure of new representatives of the huntite family, Crystal Res. Technol. 43 (2008) 157–165.